

Spin diffusion versus proximity effect at ferromagnet/superconductor $\text{La}_{0.7}\text{Ca}_{0.3}\text{MnO}_3/\text{YBa}_2\text{Cu}_3\text{O}_{7-\delta}$ interfaces

V. Peña, C. Visani, J. Garcia-Barriocanal, D. Arias,* Z. Sefrioui, C. Leon, and J. Santamaria†
GFMC, Departamento Fisica Aplicada III, Universidad Complutense de Madrid, 28040 Madrid, Spain

Carmen A. Almasan

Department of Physics, Kent State University, 105 Smith Hall, Kent, Ohio 44242, USA

(Received 14 June 2005; revised manuscript received 11 November 2005; published 27 March 2006)

We report on the interplay between magnetism and superconductivity in $\text{La}_{0.7}\text{Ca}_{0.3}\text{MnO}_3/\text{YBa}_2\text{Cu}_3\text{O}_7$ structures. We have grown heterostructures (bilayers and trilayers) with a constant thickness of the ferromagnetic layer of 40 unit cells (15 nm) and changing the thickness of the superconductor between 1 (1.2 nm) and 40 unit cells (48 nm). The critical temperature of the bilayers decreases when the thickness of the superconductor is reduced below 10 unit cells, thus providing an estimate of the length scale of superconductivity suppression by spin-polarized quasiparticles in $\text{YBa}_2\text{Cu}_3\text{O}_{7-\delta}$ (YBCO) of 10 nm, much larger than the coherence length. For thickness of the YBCO layer smaller than 4 unit cells; a second mechanism of superconductivity depression comes into play, probably related to the ferromagnetic/superconducting proximity effect. The relative importance in depressing the critical temperature of intrinsic mechanisms (quasiparticle diffusion and proximity effect) and extrinsic ones (intralayer disorder, interface roughness, or reduced dimensionality of ultrathin layers) is discussed.

DOI: [10.1103/PhysRevB.73.104513](https://doi.org/10.1103/PhysRevB.73.104513)

PACS number(s): 74.78.Fk, 74.72.Bk, 75.70.Cn

INTRODUCTION

Ferromagnetic (F) and superconducting (S) orders are antagonistic in the sense that ferromagnetism produces parallel and superconductivity antiparallel alignment of the spins. When a superconductor is placed in contact with a ferromagnet both long-range phenomena compete at the interface,^{1,2} giving rise to a variety of exotic phenomena like π junctions, spatially modulated order parameter, etc.³⁻⁵ There has been substantial activity in the past directed to study the F-S interplay in heterostructures containing transition metal superconductors (low T_c) and ferromagnets.⁶⁻¹³ In many cases the F-S competition is obscured by interface disorder like roughness, interdiffusion, or interface alloying. With the (re)discovery of colossal magnetoresistance (CMR) materials there has been renewed activity in the field with heterostructures involving high- T_c superconductors (HTSs) and CMR materials,¹⁴⁻¹⁹ which incorporate a number of interesting new ingredients. (1) F and S oxides can be chosen with the same crystalline structure, well-matching lattice parameters, and good chemical compatibility, which allows the growth of highly perfect interfaces, despite the larger complexity of these materials as compared to single-element or alloy transition metals. (2) The short coherence length of the HTSs makes superconductivity survive in very thin layers which allows examining the F-S interplay within the superconductor but very close to the interface. (3) The high degree of spin polarization of the $\text{La}_{0.7}\text{Ca}_{0.3}\text{MnO}_3$ (LCMO) conduction band together with the d -wave pairing symmetry of the superconductor make this system an adequate candidate for the search for spin-dependent effects in transport.

The F-S interaction may be understood in two different scenarios: on the one hand the Cooper pairs of the superconductor may enter the ferromagnet (proximity effect) or spins

of the ferromagnet may enter the superconductor. The latter situation will give rise to different physics depending on whether the electrons have energies larger (spin diffusion) or smaller (quasiparticle evanescent waves) than the superconducting gap. Very briefly, when a superconductor is placed in contact with a normal metal, finite pairing amplitude can be found into the normal metal at distances which may be very long at low temperatures.²⁰ However, if the normal metal is a ferromagnet, the exchange field disfavors one of the spin orientations and the distance over which superconductivity can penetrate is shortened considerably down to the 1 nm range.^{1,2} If the degree of spin polarization increases, this distance is further shortened and becomes zero for a half metal.²¹ On the other hand, when electrons of the ferromagnet with energy larger than the superconducting gap enter the superconductor, superconductivity is depressed due to breaking of the time-reversal symmetry of the Cooper pairs. The current injected from the ferromagnet is spin polarized and causes a nonequilibrium spin density to build up in the quasiparticle density of states of the superconductor, which causes the quasi Fermi levels for spin down and spin up to be displaced in opposite directions by $\delta\mu$.^{22,23} This nonequilibrium spin density affects superconductivity in a similar way as an exchange field of Zeeman energy $2\delta\mu$,²⁴ and the energy $2\delta\mu$ plays the role of a pair-breaking energy.²⁵ The degree of spin polarization of the injected current, and thus the pair-breaking effect, increases with the degree of spin polarization and is maximized for a half metal since the injected current has only one of the spin orientations. Electrons of the ferromagnet with energies smaller than the superconducting gap will enter the superconductor as quasiparticle evanescent waves.

With respect to the penetration length of spin-polarized electrons, we have to distinguish between above-gap and

below-gap energies. Electrons with energies larger than the superconducting gap will diffuse with the spin diffusion length, while electrons with energies below the gap have a characteristic penetration depth which is close to the dirty limit coherence length of the superconductor. The increased number of quasiparticles within this length scale results (self-consistently) in a suppression of the superconducting gap. This mechanism has been experimentally found to take place in permalloy/Nb heterostructures with transport measured perpendicular to the layers by Gu *et al.*²⁶ In this way, the interaction between F and S has three characteristic length scales: the coherence length of the ferromagnetic metal (proximity effect), the spin diffusion length (spin injection), and the superconducting coherence length (subgap quasiparticle diffusion), which will all typically be in the nanometer range. The study of the interplay between ferromagnetism and superconductivity at interfaces requires the growth of heterostructures with thickness of the individual layers in the range of these characteristic length scales. It is also very important to characterize the layer structure at distances to the interface comparable to the length scales of the F-S interplay to distinguish true interplay from interface-disorder-related phenomena.

In this paper we examine the F-S interplay in bilayers and trilayers made of $\text{YBa}_2\text{Cu}_3\text{O}_7$ (YBCO) and $\text{La}_{0.7}\text{Ca}_{0.3}\text{MnO}_3$. Samples show simultaneous ferromagnetism of the LCMO and superconductivity of the YBCO. Superconductivity is depressed when the YBCO thickness is reduced for constant thickness of the LCMO layers. Comparing the YBCO thickness dependence of F/S bilayers and F/S/F trilayers we find that the interplay is dominated by the proximity effect at short length scales while spin diffusion rules the T_c depression at longer length scales. We get an estimate of 10 nm for the spin diffusion length.

EXPERIMENT

Samples were grown on (100)-oriented SrTiO_3 (STO) single crystals in a high-pressure (3.4 mbar) dc sputtering apparatus at high growth temperature (900 °C). Atomic force microscopy (AFM) observations of the surface of the STO substrate showed wide flat terraces with steps of a height of 1 unit cell. The high oxygen pressure and the high deposition temperature provide a very slow (1 nm/min) and highly thermalized growth which allows the control of the deposition rate down to the unit cell limit. For this study we grew F/S bilayers and F/S/F trilayers keeping the thickness of the LCMO fixed at 40 unit cells (15 nm) and changing the thickness of the YBCO between 1 unit cell (1.2 nm) and 40 unit cells (48 nm). Structure was analyzed using x-ray diffraction and transmission electron microscopy. Further details about growth and structure can be found elsewhere.^{19,27–29} In particular transmission electron microscopy shows flat interfaces over nanometer length scales.²⁹ X-ray refinement techniques using the SUPREX 9.0 software were used to obtain quantitative information about the interface roughness at longer length scales.³⁰ T_c was measured from four-contact resistance measurements as the zero-resistance temperature in linear scale resistance plots. Mag-

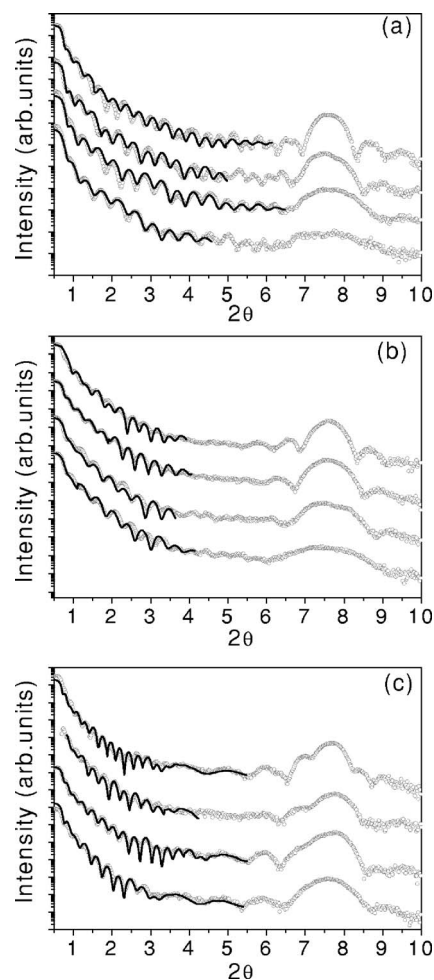


FIG. 1. Small-angle x-ray reflectivity of various bilayers with different YBCO thicknesses. Layer sequence from top layer to substrate is YBCO/LCMO/STO (a), LCMO/YBCO/STO (b), and LCMO/YBCO/PBCO/STO (c). LCMO thickness is 40 unit cell in all cases. YBCO layer thickness from bottom to top is 4, 6, 8, 10 unit cells in (a), 4, 6, 8, 10 unit cells in (b), and 2, 4, 5, 7 unit cells in (c). Lines in the figure are fits of the low-angle reflectivity using the SUPREX program (Ref. 30).

netization was measured in a superconducting quantum interference device (Quantum design) magnetometer.

RESULTS AND DISCUSSION

We have grown F/S bilayers with the YBCO on top of the LCMO (which will be referred to as YBCO/LCMO/STO bilayers) and with LCMO on top of the YBCO (which will be called LCMO/YBCO/STO bilayers). Figures 1(a) and 1(b) show small-angle reflectivity spectra of both sets of samples. Lines in the figure are fits of the low-angle reflectivity using the SUPREX program.³⁰ Due to finite-size effects the width of the 001 Bragg peak of the YBCO increases when the thickness is reduced and Laue side oscillations appear with a modulation which is directly related to thickness. YBCO layer thickness can then be obtained from the width of the Bragg peak using Scherrer's formula and from the Laue finite-size oscillations. The rapid modulation at small angle

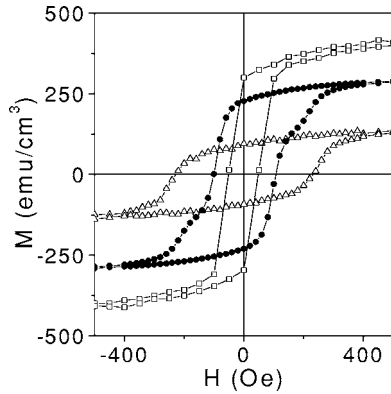


FIG. 2. Hysteresis loops at 90 K (just above the superconducting onset) after zero-field cooling of YBCO/LCMO/STO (open squares), LCMO/YBCO/PBCO/STO (open triangles), and LCMO/YBCO/LCMO/STO (solid circles). LCMO layer thickness is 40 unit cells (15.5 nm), and YBCO layer thickness is 8 unit cells (9.3 nm).

is produced by the total thickness of the sample, which allows then obtaining the thickness of the manganite layer by subtraction. It can be readily seen that for similar total thickness the number of finite-size oscillations is smaller for LCMO/YBCO/STO than for YBCO/LCMO/STO samples, evidencing a rougher F/S interface. Quantitative x-ray fitting using the SUPREX program produced roughness values of 0.4 nm for the former and 0.8 nm for the latter. This probably results from the larger lattice mismatch of YBCO ($a = 0.383$ nm, $b = 0.389$ nm) with STO (0.3905 nm) than with LCMO (0.387 nm). X-ray fitting also showed mean squared roughness values of the STO of 0.4 nm, in agreement with AFM observations showing wide flat terraces with steps of 1 unit cell in height. To improve the growth of the YBCO on the STO substrate we used a 6-unit-cell $\text{PrBa}_2\text{Cu}_3\text{O}_7$ (PBCO) buffer, which is isostructural to the YBCO though nonsuperconducting (semiconducting). In-plane lattice parameters of PBCO are about 1% larger than those of YBCO, thus providing a better epitaxy on STO. Figure 1(c) shows the x-ray reflectivity of these LCMO/YBCO/PBCO/STO samples. It is worth pointing out that the quantitative roughness analysis with the SUPREX software produced the same rms roughness values for the F/S interface of YBCO/LCMO/STO and LCMO/YBCO/PBCO/STO samples, which allows comparing the superconducting properties of both sets of samples free of the effect of interface roughness.

Figure 2 shows hysteresis loops of YBCO/LCMO/STO and LCMO/YBCO/PBCO/STO samples. It can be observed that LCMO samples grown on YBCO show depressed magnetization values as compared to layers grown directly on the STO. Figure 2 shows also data of F/S/F trilayers, where the top LCMO layer had also depressed magnetization. Furthermore, the growth on YBCO was accompanied by an increase of the Curie temperature from 208 to 250 K as observed previously by Yang *et al.*,³¹ in thicker samples. It is important to point out that the reduced magnetizations do not result from interface roughness and might be related to interface strain. Note that lattice mismatch between YBCO and LCMO, though small, is strongly anisotropic which may

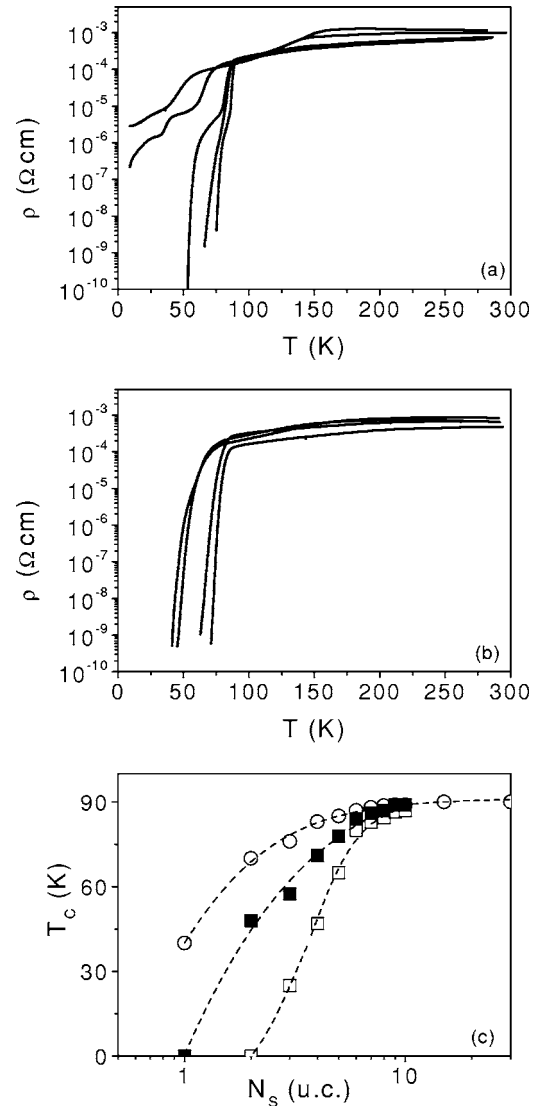


FIG. 3. Resistance curves of bilayers with different YBCO thickness. Layer sequence from top layer to substrate is YBCO/LCMO/STO (a) and LCMO/YBCO/PBCO/STO (b). YBCO layer thicknesses in the direction of increasing critical temperatures are 4, 5, 6, 8, 10 unit cells in (a), and 2, 3, 4, 5, 8 unit cells in (b). (c) T_c dependence on YBCO thickness for various samples: YBCO/LCMO/STO (open squares), LCMO/YBCO/PBCO/STO (solid squares), and reference PBCO/YBCO/PBCO trilayers (open circles).

cause inhomogeneous strain fields at the interface which may be at the origin of phase separation effects in the LCMO layers.^{32,33}

Figures 3(a) and 3(b) show resistance curves of YBCO/LCMO/STO and LCMO/YBCO/PBCO/STO samples. We have used the PBCO buffer since aside from providing a better growth as discussed above, it has been reported that YBCO single films directly grown on STO substrates have smaller T_c values as compared with samples grown in PBCO buffers.³⁴ Both samples show the critical temperature to decrease when the thickness of the superconducting layer is reduced. However, while YBCO/LCMO/STO bilayers show broad tails for the smallest YBCO thicknesses pointing to a

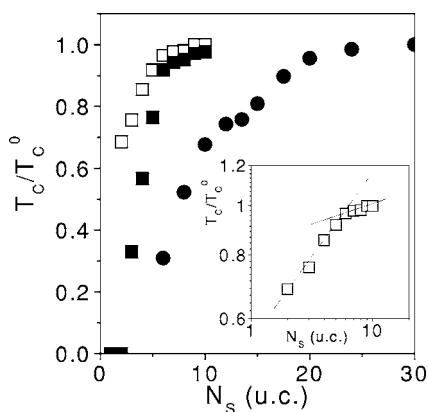


FIG. 4. T_c normalized to the critical temperature of PBCO/YBCO/PBCO trilayers of LCMO/YBCO/LCMO/STO trilayers (solid circles), LCMO/YBCO/PBCO/STO (open squares), and YBCO/LCMO/STO (solid squares) F/S bilayers as a function of YBCO thickness. Inset: log-log plot of the data corresponding to LCMO/YBCO/PBCO/STO samples.

nonhomogeneous superconductivity depression, LCMO/YBCO/PBCO/STO samples show narrower transitions. Figure 3(c) shows T_c values for both sets of samples compared with T_c of PBCO/YBCO trilayers and superlattices. It can be noticed that T_c already decreases for PBCO/YBCO structures when YBCO thickness is reduced^{35,36} as a result of epitaxial strain relaxation or dimensionality effects, but the decrease is more pronounced for samples with ferromagnetic layers as a result of the strong F/S interplay observed previously in trilayers and superlattices.^{28,29,37} Interestingly, LCMO/YBCO/PBCO/STO samples with much lower magnetization than YBCO/LCMO/STO bilayers show also higher T_c values for the same thickness values of the individual YBCO layers, which further supports the role played by the interplay between ferromagnetism and superconductivity in depressing the critical temperature in these samples.

To rule out growth-related effects like disorder or roughness of the YBCO layer, it is interesting to examine the depression of the critical temperature in F/S/F trilayers of the same thickness of the YBCO and LCMO layers as in F/S bilayers. If the T_c depression were caused by disorder, reduced dimensionality or any other process within the YBCO layer, one would expect the T_c to be the same for trilayers as for bilayers. If on the other hand the T_c depression is due to processes originating at the YBCO/LCMO interface like spin diffusion or the F/S proximity effect, twice the thickness of YBCO is required in trilayers to produce the same T_c change as in the corresponding bilayer. Figure 4 shows the evolution of the ratio T_c/T_c^0 of T_c over the critical temperature T_c^0 of PBCO/YBCO/PBCO samples, for bilayers and F/S/F trilayers as a function of YBCO thickness. Data corresponding to two different bilayers, LCMO/YBCO/PBCO/STO (open squares) and YBCO/LCMO/STO (solid squares), have been included in Fig. 4. The thickness of the LCMO layer is 40 unit cells in all cases. It can be observed that roughly twice the thickness of the YBCO is necessary for LCMO/YBCO/LCMO trilayers to have the same T_c as YBCO/LCMO/STO bilayers, pointing to interface processes like spin diffusion or the F/S proximity effect as possible causes for T_c depression.

Notice also that the bulk T_c is recovered for 10-unit-cell-thick YBCO and that 20-unit-cell-thick layers are necessary in the case of trilayers. It is worth pointing out that since the magnetization of LCMO layers grown on top of YBCO is depressed as compared with LCMO grown directly on STO, LCMO/YBCO/PBCO/STO bilayers (open squares in Fig. 4) show larger T_c than YBCO/LCMO/STO (solid squares) for the same YBCO thickness, and thus somewhat longer than twice the YBCO thickness is necessary to get the T_c of the trilayers. In view of the high degree of spin polarization of the LCMO, and since Andreev reflection, and consequently the proximity effect, does not occur in a half metal, effects due to spin injection are expected to dominate over those related to the proximity effect. However, we have recently reported indications of a proximity effect in these samples extending distances of 5 nm into the ferromagnet.²⁹ We provide here further support for the existence of a proximity effect in bilayers with small thickness of the superconducting layer. Due to the good epitaxial properties of YBCO, PBCO, and LCMO, we can compare the critical temperature of F/S bilayers with and without a PBCO barrier between the F and the S materials. The presence of the semiconducting PBCO spacer will certainly suppress two-particle transport (i.e., proximity effect) although single electrons will still find a small resistance to tunnel through.³⁸ Figure 5 shows a comparison of resistance curves of samples with and without a 6-unit-cell-thick PBCO spacer between F and S layers, for various YBCO thicknesses. It can be observed that significant (partial) recovery of the critical temperature occurs for very thin YBCO layers pointing to the existence of a different mechanism of superconductivity suppression taking place at short length scales, which may be an indication of the proximity effect. Moreover, the recovery of the critical temperature when insulating PBCO is introduced between F and S layers is no longer observed in samples with thicker YBCO, what is also consistent with the proximity effect scenario, since the critical temperature is less influenced by proximity effect when the thickness of the superconducting layer increases. In the framework of the F/S proximity effect, no matter the thickness of the ferromagnetic layer, the bulk T_c remains basically unaffected for superconducting layers of thickness d_S , larger than roughly ten times the Ginzburg-Landau coherence length $\xi_S(0)$,¹ which is very short in this superconductor (0.1–0.3 nm). Therefore no depression of the critical temperature originating at the F/S proximity effect is expected for YBCO thickness values larger than 4 unit cells. The inset of Fig. 4 shows a log-log plot of the critical temperature as a function of YBCO thickness, where the kink at 5 unit cells suggests that in fact a second mechanism may be ruling the T_c depression at small YBCO layer thickness. The depressed magnetization found in the LCMO layers grown on top of YBCO provides a physically reasonable basis for the existence of a proximity effect. If the sample consists of isolated ferromagnetic regions separated by distances longer than the coherence length of the ferromagnet superconductivity may penetrate nonhomogeneously into the LCMO along these nonferromagnetic regions. In summary, we find indications of the F/S proximity effect acting to depress T_c at low YBCO thickness, although we cannot rule out other charge transfer phenomena taking place at the interface

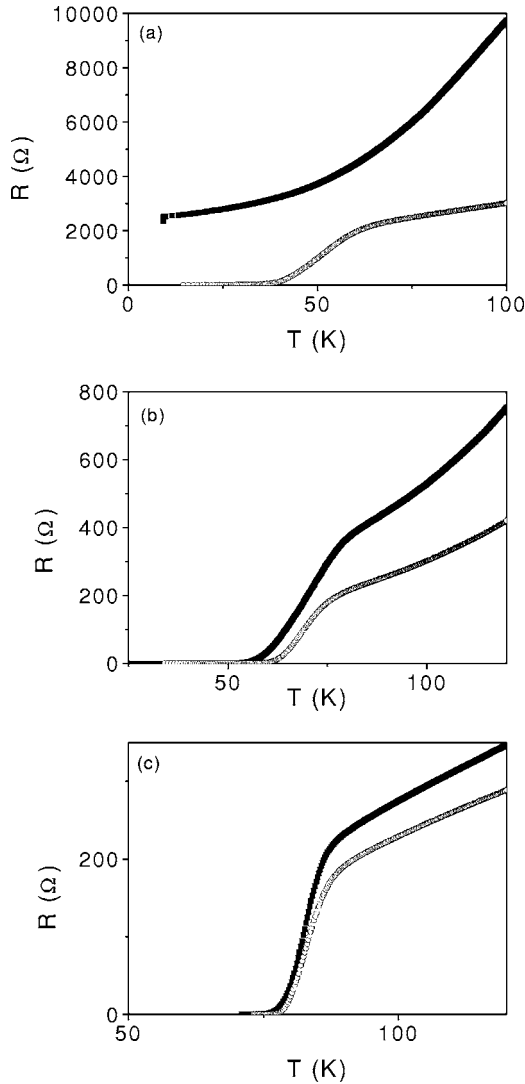


FIG. 5. Resistance curves of LCMO/YBCO/PBCO/STO bilayers (solid symbols) and same samples with a 6-unit-cell-thick PBCO spacer between F and S layers. YBCO thickness are 1 (a), 3 (b), and 5 (c) unit cells.

as a result of band bending or polarity mismatch. We have recently found from atomic resolution electron energy loss spectroscopy that significant electron transfer occurs from the manganite into the YBCO.³⁹ As a result, the density of holes is depressed over roughly 3 unit cells from the interface, which will certainly also affect the critical temperature of the YBCO at the interface. Introducing a PBCO spacer will also limit this charge transfer mechanism providing an additional mechanism for the T_c recovery observed in Fig. 5. At present we cannot assess the relative importance of charge transfer and proximity effect. Note from the inset of Fig. 4 that significant T_c depression is still observed for layer thickness above 5 unit cells both for bilayers and for trilayers (see Fig. 4) pointing to quasiparticles as the source of pair breaking for this YBCO thickness range. This, of course, does not mean that (single) quasiparticle penetration does not affect T_c for thinner YBCO, but the effect of proximity seems to be superimposed. Since the bulk T_c is recovered for 10-unit-cell YBCO layer thickness in F/S bilayers and

roughly for 20-unit-cell-thick layers in F/S/F trilayers, we can estimate a length scale of 10 nm ruling superconductivity suppression into the YBCO in this system.

Now we discuss the relative importance of quasiparticles with energies above or below the superconducting gap in depressing the critical temperature. At or close to T_c a fraction of spin-polarized quasiparticles will exist with energies around or below the gap value, and these will have a penetration depth of the order of ξ_S which diverges at T_c [$\xi_S(T) = \xi_S(0)/(1 - T/T_c)^{1/2}$]. The number of quasiparticles decreases when gap size is increased, i.e., when temperature is decreased. Thus when the thickness of the superconductor is increased beyond the length scale of the depressed gap by the proximity effect, this will also reduce the number of evanescent quasiparticles since their accessible energy range becomes narrower. Gap suppression by evanescent quasiparticles is then a physical scenario to discuss the superconductivity depression when the YBCO thickness is reduced. However, note that close to T_c the fraction of quasiparticles with energy lower than the gap will be small, and therefore this mechanism is expected to be dominant at low temperatures as experimentally found by Gu *et al.*²⁶ In our measurement geometry the current flows in the plane of the layers; therefore spin diffusion from the LCMO layer into the YBCO may result from self-diffusion or from electron scattering within the ferromagnetic layers. LCMO is a relatively bad metal and many collision events will result in electrons being scattered into the YBCO. These electrons will be highly spin polarized and are expected to cause T_c depression by pair breaking as previously discussed by other authors^{40–42} if the YBCO thickness is smaller than the spin diffusion length, l_S . An estimate of l_S in YBCO can be obtained using the relation $l_S = (l_0 v_F \tau_S)^{0.5}$,⁴¹ where τ_S is the spin-polarized quasiparticle diffusion time, v_F is the Fermi velocity, and l_0 is the electron mean free path. τ_S can be estimated by the relation $\tau_S \sim 3.7 \hbar k_B T_c / E_{ex} \Delta(T)$, where $E_{ex} \sim 30$ K is the average on-site spin exchange interaction in YBCO and $\Delta(T) = \Delta(0)(1 - T/T_c)^{0.5}$ is the temperature-dependent gap. Assuming a value of $\tau_S = 10^{-13}$ s,⁴¹ $v_F = 10^7$ cm/s and that the electron mean free path of YBCO is $l_0 = 20$ nm, l_S can be of the order of 14 nm, in agreement with the 10 nm estimated recently by Soltan *et al.*⁴³ This work also reports on LCMO/YBCO bilayers although focusing on much thicker YBCO layer thickness.

In summary, from our experiments on bilayers and trilayers made of highly spin-polarized LCMO and high- T_c superconducting YBCO we have found two mechanisms for T_c depression at the interface. One occurring at short length scales (YBCO thickness smaller than 5 unit cells) might be related to a F/S proximity effect and the other occurring at longer length scales is most likely due to pair breaking by spin-polarized carriers entering the superconductor. The dependence of the T_c of F/S heterostructures on the thickness of the superconducting layer has allowed us to get an estimate for the length scale of superconductivity suppression by spin-polarized quasiparticles in the YBCO of 10 nm. At present we cannot ascertain whether evanescent quasiparticles with energies below the superconducting gap or spin

diffusion with energies larger than the gap are responsible for the long-length-scale superconductivity depression. Experiments with the current directed perpendicular to the layers will help to clarify this point.

ACKNOWLEDGMENTS

This work was supported by MCYT MAT 2005-06024 and CAM GR-MAT-0771/2004.

*On leave from Universidad del Quindío, Armenia, Colombia.

†Corresponding author. Email address: jacsan@fis.ucm.es

- ¹Z. Radovic, L. Dobrosavljevic-Grujic, A. I. Buzdin, and J. R. Clem, *Phys. Rev. B* **38**, 2388 (1988); Z. Radovic, M. Ledvij, L. Dobrosavljevic-Grujic, A. I. Buzdin, and J. R. Clem, *ibid.* **44**, 759 (1991); I. Baladić and A. Buzdin, *ibid.* **67**, 014523 (2003).
- ²A. I. Buzdin, *Rev. Mod. Phys.* **77**, 935 (2005); F. S. Bergeret, A. F. Volkov, and K. B. Efetov, *ibid.* **77**, 1321 (2005).
- ³V. V. Ryazanov, V. A. Oboznov, A. Y. Rusanov, A. V. Veretennikov, A. A. Golubov, and J. Aarts, *Phys. Rev. Lett.* **86**, 2427 (2001).
- ⁴T. Kontos, M. Aprili, J. Lesueur, F. Genêt, B. Stephanidis, and R. Boursier, *Phys. Rev. Lett.* **89**, 137007 (2002).
- ⁵A. Buzdin and I. Baladić, *Phys. Rev. B* **67**, 184519 (2003).
- ⁶C. Uher, R. Clarke, G. G. Zheng, and I. K. Schuller, *Phys. Rev. B* **30**, 453 (1984).
- ⁷J. Aarts, J. M. E. Geers, E. Brück, A. A. Golubov, and R. Coehoorn, *Phys. Rev. B* **56**, 2779 (1997).
- ⁸Th. Mühge, N. N. Garif'yanov, Yu. V. Goryunov, G. G. Khaliullin, L. R. Tagirov, K. Westerholt, I. A. Garifullin, and H. Zabel, *Phys. Rev. Lett.* **77**, 1857 (1996).
- ⁹L. V. Mercaldo, C. Attanasio, C. Coccorese, L. Maritato, S. L. Prischepa, and M. Salvato, *Phys. Rev. B* **53**, 14040 (1996).
- ¹⁰J. S. Jiang, Dragomir Davidovic, Daniel H. Reich, and C. L. Chien, *Phys. Rev. B* **54**, 6119 (1996).
- ¹¹A. Yu. Rusanov, M. Hesselberth, J. Aarts, and A. I. Buzdin, *Phys. Rev. Lett.* **93**, 057002 (2004).
- ¹²G. Verbanck, C. D. Potter, V. Metlushko, R. Schad, V. V. Moshchalkov, and Y. Bruynseraede, *Phys. Rev. B* **57**, 6029 (1998).
- ¹³L. Lazar, K. Westerholt, H. Zabel, L. R. Tagirov, Yu. V. Goryunov, N. N. Garifyanov, and I. A. Garifullin, *Phys. Rev. B* **61**, 3711 (2000).
- ¹⁴G. Jakob, V. V. Moshchalkov, and Y. Bruynseraede, *Appl. Phys. Lett.* **66**, 2564 (1995).
- ¹⁵P. Przyslupski, S. Kolesnik, E. Dynowska, T. Skoskiewicz, and M. Sawicki, *IEEE Trans. Appl. Supercond.* **7**, 2192 (1997).
- ¹⁶C. A. R. Sá de Melo, *Phys. Rev. Lett.* **79**, 1933 (1997); *Phys. Rev. B* **62**, 12303 (2000).
- ¹⁷P. Prieto, P. Vivas, G. Campillo, E. Baca, L. F. Castro, M. Varela, C. Ballesteros, J. E. Villegas, D. Arias, C. Leon, and J. Santamaría, *J. Appl. Phys.* **89**, 8026 (2001).
- ¹⁸H.-U. Habermeier, G. Cristiani, R. K. Kremer, O. I. Lebedev, and G. Van Tendeloo, *Physica C* **354**, 298 (2001).
- ¹⁹Z. Sefrioui, M. Varela, V. Peña, D. Arias, C. Leon, J. Santamaría, J. E. Villegas, J. L. Martinez, W. Saldarriaga, and P. Prieto, *Appl. Phys. Lett.* **81**, 4568 (2002).
- ²⁰For a review see C. W. J. Beenakker, *Rev. Mod. Phys.* **69**, 731 (1997).
- ²¹M. J. M. de Jong and C. W. J. Beenakker, *Phys. Rev. Lett.* **74**, 1657 (1995).
- ²²M. Johnson and R. H. Silsbee, *Phys. Rev. Lett.* **55**, 1790 (1985).
- ²³M. Jonson, *Appl. Phys. Lett.* **65**, 1460 (1994).
- ²⁴S. Takahashi, H. Imamura, and S. Maekawa, *Phys. Rev. Lett.* **82**, 3911 (1999).
- ²⁵G. Sarma, *J. Phys. Chem. Solids* **24**, 1029 (1963).
- ²⁶J. Y. Gu, J. A. Caballero, R. D. Slater, R. Loloee, and W. P. Pratt, Jr., *Phys. Rev. B* **66**, 140507R (2002).
- ²⁷Z. Sefrioui, D. Arias, V. Peña, J. E. Villegas, M. Varela, P. Prieto, C. León, J. L. Martínez, and J. Santamaría, *Phys. Rev. B* **67**, 214511 (2003).
- ²⁸V. Peña, Z. Sefrioui, D. Arias, C. León, J. L. Martínez, and J. Santamaría, *Eur. Phys. J. B* **40**, 479 (2004).
- ²⁹V. Peña, Z. Sefrioui, D. Arias, C. Leon, J. Santamaría, M. Varela, S. J. Pennycook, and J. L. Martinez, *Phys. Rev. B* **69**, 224502 (2004).
- ³⁰Small-angle reflectivity profiles are calculated applying a recursive Fresnel formalism as described by J. H. Underwood and T. W. Barbee, *Appl. Opt.* **20**, 3027 (1981). Details about the calculation method can be found in I. K. Schuller, *Phys. Rev. Lett.* **44**, 1597 (1980); W. Sevenhans, M. Gijjs, Y. Bruynseraede, H. Homma, and I. K. Schuller, *Phys. Rev. B* **34**, 5955 (1986); E. E. Fullerton, I. K. Schuller, H. Vanderstraeten, and Y. Bruynseraede, *ibid.* **45**, 9292 (1992); D. M. Kelly, E. E. Fullerton, J. Santamaría, and I. K. Schuller, *Scr. Metall. Mater.* **33**, 1603 (1995).
- ³¹Z. Q. Yang, R. Hendrikx, J. Aarts, Y. Qin, and H. W. Zandbergen, *Phys. Rev. B* **67**, 024408 (2003).
- ³²K. H. Ahn, T. Lookman, and A. R. Bishop, *Nature (London)* **428**, 401 (2004).
- ³³E. Dagotto, T. Hotta, and A. Moreo, *Phys. Rep.* **344**, 1 (2001).
- ³⁴M. Varela, W. Grogger, D. Arias, Z. Sefrioui, C. León, L. Vazquez, C. Ballesteros, K. M. Krishnan, and J. Santamaría, *Phys. Rev. B* **66**, 174514 (2002).
- ³⁵M. Varela, Z. Sefrioui, D. Arias, M. A. Navacerrada, M. Lucía, M. A. López de la Torre, C. León, G. D. Loos, F. Sanchez-Quesada, and J. Santamaría, *Phys. Rev. Lett.* **83**, 3936 (1999).
- ³⁶M. Varela, W. Grogger, D. Arias, Z. Sefrioui, C. León, C. Ballesteros, K. M. Krishnan, and J. Santamaría, *Phys. Rev. Lett.* **86**, 5156 (2001).
- ³⁷V. Peña, Z. Sefrioui, D. Arias, C. Leon, J. Santamaría, J. L. Martínez, S. G. E. teVelthuis, and A. Hoffmann, *Phys. Rev. Lett.* **94**, 057002 (2005).
- ³⁸R. J. Soulen, J. M. Byers, M. S. Osofski, B. Nadgorny, T. Ambrose, S. F. Cheng, P. R. Broussard, C. T. Tanaka, J. Nowak, J. S. Moodera, A. Barry, and J. M. D. Coey, *Science* **282**, 85 (1998).
- ³⁹M. Varela, A. R. Lupini, V. Peña, Z. Sefrioui, I. Arslan, N. D. Browning, J. Santamaría, and S. J. Pennycook (unpublished).
- ⁴⁰V. A. Vas'ko, V. A. Larkin, P. A. Kraus, K. R. Nikolaev, D. E. Grupp, C. A. Nordman, and A. M. Goldman, *Phys. Rev. Lett.* **78**, 1134 (1997); A. M. Goldman, V. A. Vas'ko, P. Kraus, K.

- Nikolaev, and V. A. Larkin, *J. Magn. Magn. Mater.* **200**, 69 (1999).
- ⁴¹N. C. Yeh, R. P. Vasquez, C. C. Fu, A. V. Samoilov, Y. Li, and K. Vakili, *Phys. Rev. B* **60**, 10522 (1999).
- ⁴²Y. Gim, A. W. Kleinsasser, and J. B. Barner, *J. Appl. Phys.* **90**, 4063 (2001).
- ⁴³S. Soltan, J. Albrecht, and H.-U. Habermeier, *Phys. Rev. B* **70**, 144517 (2004).